ARL-TR-8887 ● JAN 2020

DEVCOM ARMY RESEARCH LABORATORY

Sample Preparation Methods for Diamond–Silicon-Carbide Microstructure Analysis

by Jonathan P Ligda, Taylor Shoulders, and Anthony DiGiovanni

NOTICES

Disclaimers

The findings in this report are not to be construed as an official Department of the Army position unless so designated by other authorized documents.

Citation of manufacturer's or trade names does not constitute an official endorsement or approval of the use thereof.

Destroy this report when it is no longer needed. Do not return it to the originator.

ARL-TR-8887 ● JAN 2020

Sample Preparation Methods for Diamond–Silicon-Carbide Microstructure Analysis

Jonathan P Ligda, Taylor Shoulders, and Anthony DiGiovanni
Weapons and Materials Research Directorate, CCDC Army Research Laboratory

REPORT DOCUMENTATION PAGE

Form Approved
OMB No. 0704-0188

1. REPORT DATE *(DD-MM-YYYY)*	2. REPORT TYPE	3. DATES COVERED (From - To)
January 2020	Technical Report	1 July–17 Sept 2019

4. TITLE AND SUBTITLE
Sample Preparation Methods for Diamond-Silicon Carbide Microstructure Analysis

5a. CONTRACT NUMBER

5b. GRANT NUMBER

5c. PROGRAM ELEMENT NUMBER

6. AUTHOR(S)
Jonathan P Ligda, Taylor Shoulders, and Anthony DiGiovanni

5d. PROJECT NUMBER

5e. TASK NUMBER

5f. WORK UNIT NUMBER

7. PERFORMING ORGANIZATION NAME(S) AND ADDRESS(ES)
CCDC Army Research Laboratory
ATTN: FCDD-RLW-MB
Aberdeen Proving Ground, MD 21005

8. PERFORMING ORGANIZATION REPORT NUMBER
ARL-TR-8887

9. SPONSORING/MONITORING AGENCY NAME(S) AND ADDRESS(ES)

10. SPONSOR/MONITOR'S ACRONYM(S)

11. SPONSOR/MONITOR'S REPORT NUMBER(S)

12. DISTRIBUTION/AVAILABILITY STATEMENT
Approved for public release; distribution is unlimited.

13. SUPPLEMENTARY NOTES
ORCID ID: Jonathan P Ligda, 0000-0003-3539-8867

14. ABSTRACT

Microstructural characterization of diamond-containing ceramic composites, like diamond–silicon carbide (SiC), requires advanced sample preparation methods. Tradition mechanical polishing methods cannot be used due to the addition of diamond particles. Instead, techniques like the scaife process for diamond knife polishing, ion polishing, or laser polishing must be used. In this report a diamond–SiC composite, polished using these three methods is characterized using scanning electron microscopy (SEM), Raman spectroscopy, and electron backscatter diffraction (EBSD). This report shows which polishing methods are sufficient to acquire data for each characterization technique. While the scaife process is the best method for polishing diamond–SiC, all characterization techniques are feasible over a large area. Ion polishing is also capable of polishing this material well enough for each characterization technique, but only over small areas. Laser polishing is sufficient enough for SEM and Raman but too textured for accurate EBSD.

15. SUBJECT TERMS
diamond, polishing, scanning electron microscopy, SEM, Raman, electron backscatter diffraction, EBSD

16. SECURITY CLASSIFICATION OF:			17. LIMITATION OF ABSTRACT	18. NUMBER OF PAGES	19a. NAME OF RESPONSIBLE PERSON
a. REPORT	b. ABSTRACT	c. THIS PAGE			Jonathan P Ligda
Unclassified	Unclassified	Unclassified	UU	18	19b. TELEPHONE NUMBER (Include area code) 410-306-4786

Contents

List of Figures

List of Tables

1. Introduction

The reduction in cost for some grades of synthetic diamond grit has reached about $0.10 per carat, enabling its high-volume-fraction inclusion in advanced composite ceramic systems an economically viable consideration.[1] One current commercially available composite under consideration is diamond–silicon carbide (SiC).[2,3] This composite ceramic exhibits an increase in hardness and fracture toughness compared with SiC and boron carbide while maintaining a similar density.[4] The combination of these properties make diamond–SiC composites an attractive material for use as an armor ceramic. However, a more detailed, multiscale study on how the interface between diamond and SiC influences the mechanical/ballistic behavior is needed to determine an optimized microstructure for improving dynamic performance. Properly studying these interfaces requires a coordinated effort among processing, modeling, and characterization components. Both commercial and in-house ceramic composites will require microstructural characterization through a combination of scanning electron microscopy (SEM), electron backscatter diffraction (EBSD), energy dispersive spectroscopy (EDS), Raman spectroscopy, and transmission electron microscopy, which require polished surfaces. However, the addition of diamond in this ceramic composite presents a challenge for microstructure characterization techniques because traditional ceramic polishing procedures involve the use of diamond as the polishing media. Polishing the diamond phase concurrently with the SiC phase requires special methods.

Historically, the diamond polishing technique known as the scaife process has evolved from the gemstone industry.[5,6] In this process, the diamond sample to be polished is pressed, at loads of roughly 2.0 MPa, against a rotating cast iron disc loaded with diamond grit. This process is highly anisotropic, with diamond displaying “hard” and “soft” orientations; material removal rates in the “soft” direction can be near tens of nanometers/hour depending on the rotation speed and pressure. The mechanism for material removal is reported to be a mechanically induced phase transition from sp3 to sp2 carbon (i.e., diamond to graphite). The graphitized carbon is then easily removed by the imbedded diamond grit in the cast iron wheel. Improvements can be made by introducing an oxidizing agent to the wheel for chemical mechanical polishing or high temperatures for thermo-chemical polishing. Other nonmechanical polishing techniques such as ion beam or laser polishing are also capable of polishing diamond. Ion beam polishing uses a broad (unfocused) beam of ions, typically argon, accelerated at 3–10 kV and directed toward a sample.[7] This process is capable of polishing diamond–SiC composites, but only over a small area. Laser-based shaping and polishing systems have seen

ever-increasing use in the diamond industry owing to the cost savings realized from reduced material loss and increased throughput.[8,9] Laser-based systems can be configured to process all forms of bulk diamond, including gem, polycrystalline diamond, polycrystalline diamond compacts, and chemical vapor deposited (CVD) materials. Pimenov et. al. used copper vapor and argon fluoride excimer lasers to polish CVD diamond films, finding that it is possible to polish the rough growth surface and remove a defect layer from surfaces.[10,11] Femtosecond lasers have also been considered for polishing diamond surfaces but have been shown to create submicron features known as laser-induced periodic surface structures (LIPSSs) on diamond crystals.[12,13] These structures are ripples on the surface that have a periodicity on the order of the wavelength of the laser.[14–16]

For this study, a commercial, reaction-bonded diamond–SiC composite is used to study different diamond–SiC surface preparation methods. The goal is to determine if any other method could provide some basic microstructural information since the scaife process is not available in-house at the US Army Combat Capabilities Development Center Army Research Laboratory and can take weeks to receive a finished sample. A variety of material and microstructure properties are needed from this material, including diamond particle size, SiC grain size, SiC phase identification, and grain boundary types. Therefore, the characterization techniques focused on here will be SEM, EBSD/EDS, and Raman spectroscopy.

2. Experimental

A commercially available reaction-bonded diamond–SiC sample with 21% diamond by volume was obtained from Mcubed. This sample is a 100- × 100- × 10-mm plate with a density of 3.21 g/cm^3. The plate was sent to Applied Diamond for laser sectioning and mechanical polishing (scaife process). Applied Diamond specializes in mechanical polishing of diamond, but an updated process must be determined for the composite due to the addition of a SiC matrix phase. Additionally, broad-beam ion polishing and femtosecond laser milling are completed to determine the effectiveness of any in-house capabilities. For ion polishing, a Leica TIC-3X is used with 1- to 2-mm-thick sections in a cross-section geometry and polished at 8 kV/3 mA for 10 h. The laser used for this work is a Clark-MXR CPA femtosecond laser, which has a wavelength of 775 nm and a pulse width of 150–200 fs. Samples were polished with pulse energy of 15 μJ, 1 mm/s scan speed, and a line width of 20 μm. All the laser milling is done with the laser at a normal incidence to the surface.

Once polished, each sample was characterized to determine if the surface quality was sufficient to get the desired microstructural information. Initial SEM images

were taken with a Phenom XL desktop SEM in backscatter mode, which provides good contrast between the diamond and SiC phases. From these images, the size and number of diamond particles were determined using ImageJ. Raman spectroscopy of the polished surfaces was done using a Horiba LabRam HR Evolution at a wavelength of 633 nm with a 100× objective and a 10-s exposure time over five iterations. Since phase identification and residual stress are most important in the matrix regions, all Raman scans are done in the SiC phase and focus on the range of 750–850 cm^{-1}, where vibrations characteristic of the common 3C, 6H, and 15R polytypes are found. Orientation relationships at grain and phase boundaries are of interest: attempts at EBSD mapping are done using an EDAX Hikari camera, attached to an FEI NanoSEM operating at 20 kV, 1.5 nA, with a step size of 500 nm. The data were postprocessed using a grain-based confidence index (CI) standardization followed by a single iteration of neighbor CI correlation to clean up the orientation maps.

Each characterization technique has its own quantitative metric used to determine the effectiveness of a given polishing method. The size and standard deviation of the diamond particles are used for the SEM images. The presence and location of peaks compared with literature values are the quantitative metric used for Raman spectroscopy. The scanned range covers the primary transverse optical mode for 3C SiC as well as the folded modes characteristic of other SiC polytypes. For EBSD, the maps provide a few quantitative values for comparison, including CI, image quality (IQ), and fit.

3. Results

Backscatter SEM images from all three polishing methods are shown in Figs. 1a–1c. The dark phase in these images are diamond particles, while the lighter phase is the SiC. Each polished surface provides a sufficient backscattered electron yield to qualitatively identify the different phases. However, there are differences when attempting to measure the diamond particle sizes, as shown in Table 1. The ImageJ analysis shows that diamond particle sizes are 14.78 ± 8.01, 16.54 ± 9.73, and 18.51 ± 8.63 μm for the mechanical-, laser-, and ion-polished surfaces, respectively. These are comparable values among the polishing techniques, and each provides a sufficiently large number of particles for counting. The best statistics for particle measurements are from the mechanical or laser polishing simply because these methods polish the largest areas. However, care must be taken with laser-polished surfaces due to the formation of LIPSSs. Shown in Fig. 2, these LIPSSs have a periodicity on the order of the wavelength of the laser, 762 ± 246 nm. While the depth of these structures is on the order of nanometers, they are still evident during image thresholding and therefore influence the ImageJ

particle measurements. However, these features are small and have a high aspect ratio; as such, they can be accounted for by limiting measurements to only including larger, more-circular particles.

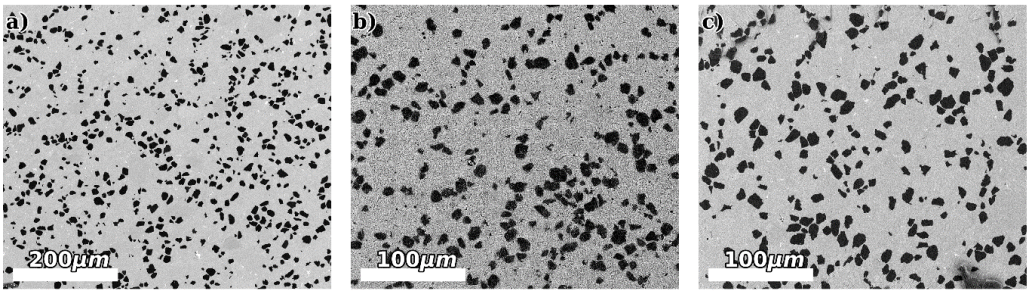

Fig. 1 Backscatter SEM images from surfaces polished using the a) scaife process, b) femtosecond laser, and c) broad-beam ion polisher. The darker phases are the diamond particles.

Table 1 Diamond particle diameter and number of particles counted for each polishing method

Method	Diameter (µm)	No. of particles
Mechanical	14.78 ± 8.01	544
Laser	16.54 ± 9.73	299
Ion	18.51 ± 8.63	261

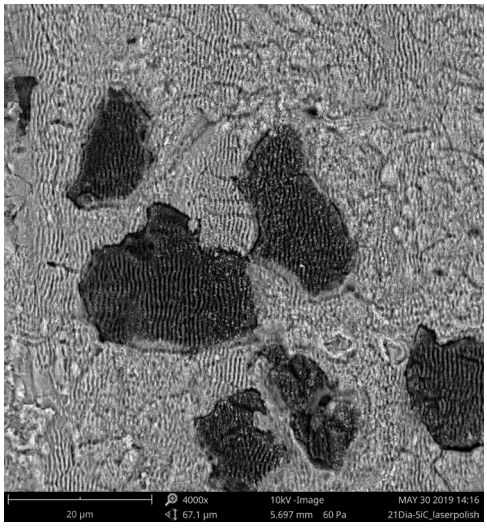

Fig. 2 Backscatter SEM image from the femtosecond laser-polished sample showing the presence of LIPSSs in both phases

Each polishing method is also capable of producing a surface quality sufficient for Raman spectroscopy. Figures 3a–c show the Raman spectra from each polishing method in the wavenumber range of 750–850 cm^{-1}. These peaks correspond to the E_1(TO) and E_2 planar Raman modes for 6H-SiC. The biggest difference between these scans is the higher overall intensity of the mechanically polished surface in Fig. 3a over the laser polish in Fig. 3b and ion polish in Fig. 3c. Work from Beard et. al.[17] showed that there is a reduction in Raman intensity with increasing surface roughness, indicating the LIPSSs discussed previously contribute to the reduction in intensity for the laser-polished surface.

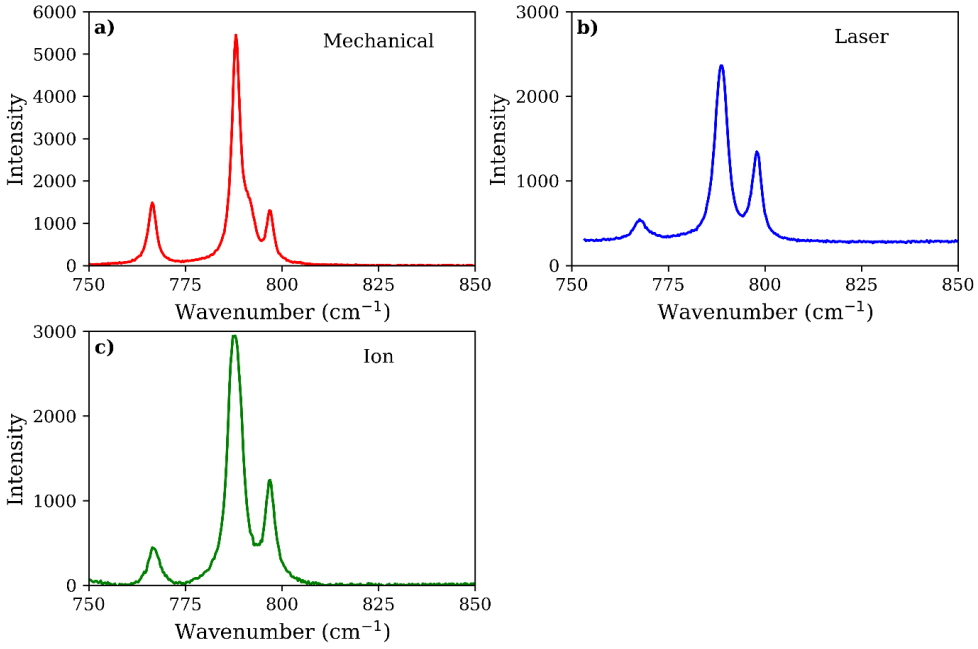

Fig. 3 Raman spectra in the range of 750–850 cm^{-1} for all three polishing methods: a) mechanical, b) laser, and c) ion. All show the expected SiC peaks without any major shifts in peak position.

However, the LIPSSs and laser milling do not have an effect on the position of the Raman peaks. For all polishing methods, the measured peak positions do not vary much compared with these literature values, as shown in Table 2. For the mechanically polished sample there is only an average percent error of 0.08% between the literature and measured peak positions. For the laser- and ion-polished surfaces, the average percent error is 0.107% and 0.089%, respectively.

Table 2 Measured Raman peak positions for each polishing method and the literature values for the same peaks. The laser polish has no large effect on the position of the Raman peaks.

Method	Peak positions (cm^{-1})		
Literature	767.5	788	796
Mechanical	766.409	788.046	796.732
Laser	767.558	788.598	797.883
Ion	766.425	787.874	796.905

Results from the EBSD scans are shown in Figs. 4a–4f. Inverse pole figure (IPF) and phase identification (ID) maps from the mechanical- and ion-polished samples are shown Figs. 4a–4b and Figs. 4c–4d, respectively. The IPF triangle key and phase color legend are indicated in Fig. 4e. These are the only polishing methods capable of providing EBSD data. As shown in the SEM image in Fig. 4f, there is texturing on the laser-polished surface that limits collection of EBSD data. The texturing does not actually impede electron diffraction from this surface. Rather, it blocks the diffracted beam from reaching the camera, making it impossible to index accurately.

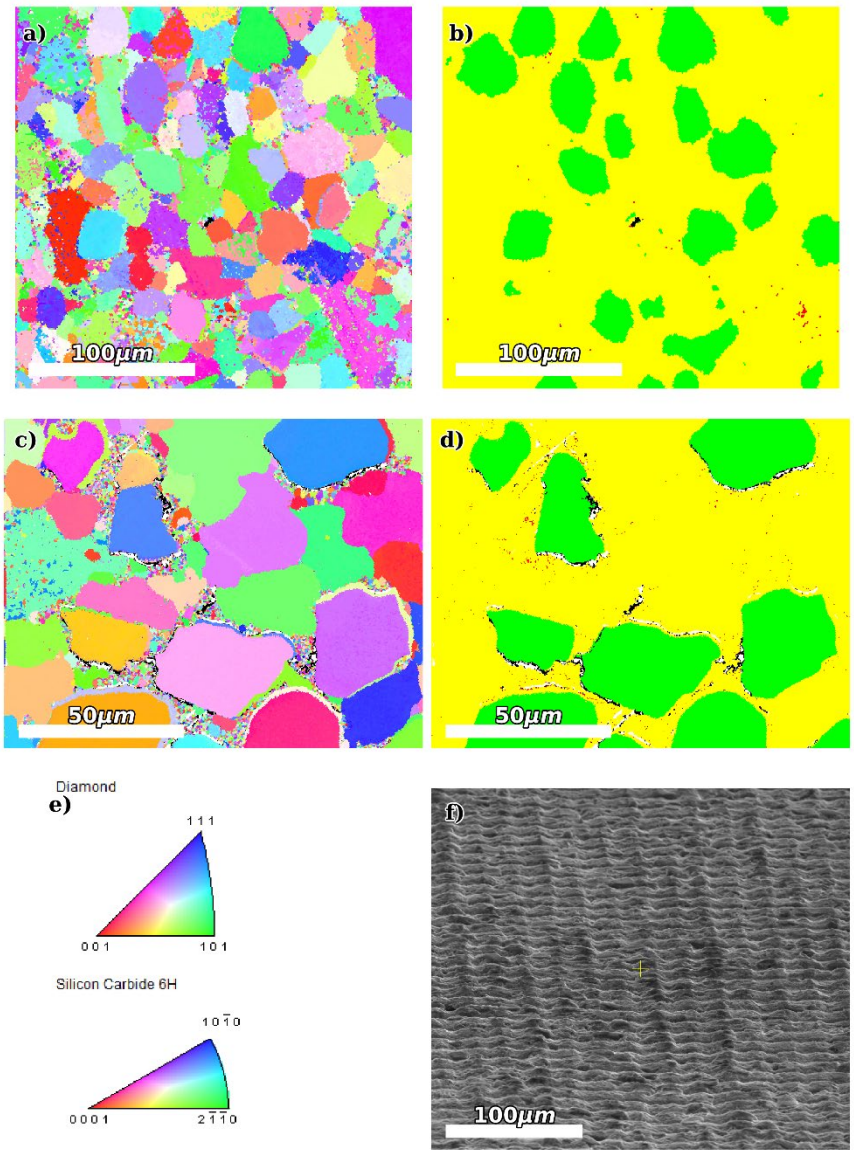

Fig. 4 EBSD results for the polishing methods, (a–e). Only the mechanical polish and ion polished surfaces were capable of providing EBSD data. The laser polished surface (f) is too rough, which blocks any diffracted beam from the camera.

For both polishing methods, the diamond and SiC phases show clean diffraction patterns. The mechanically polished surface has an average CI = 0.25, IQ = 6380.17, and fit of 1.86°. The ion-polished surface has an average CI = 0.54, IQ = 1879.05, and fit of 1.59°. For reference, a recent map on a nickel sample used for EBSD calibration had an average CI = 0.59, IQ = 4599.03, and fit of 1.01°. Note that to improve the indexing of both phases, EBSD should be run concurrently with EDS, which, while not shown here, is possible on surfaces from all polishing methods. This is important because some diamond–SiC materials contain the cubic

diamond phase along with the cubic 3C SiC phase. This makes the traditional EBSD indexing procedure difficult, but the combination of these two techniques allows the analysis software to use the chemical information provided by EDS to rule out phases during indexing.

4. Discussion and Conclusions

The addition of diamond into a ceramic composite system, such as diamond–SiC, requires special sample preparation techniques for microstructure characterization. Traditional diamond polishing techniques, such as the scaife method, are capable of polishing this ceramic composite, but more-advanced techniques like ion or laser polishing are also practical, depending on the characterization needed. Table 3 is an overview of each polishing method and whether or not the corresponding characterization technique is accomplished. For SEM imaging, all three methods provide an adequate surface finish for observing and measuring the diamond particle locations and sizes as well as a qualitative description of the SiC phase. While the scaife process provides the largest polished area for observation, the ion polish provides the smallest. Raman spectroscopy is possible from all polishing methods as well; however, care must be taken to not create a significant amount of texturing with the laser polishing because it could affect the signal. For EBSD, only the mechanical and ion polishing were able to provide accurate maps.

Table 3 Overview of characterization techniques available following the corresponding sample polish method. The mechanical polish gives the best results over the largest area.

Polishing method	Characterization technique		
	SEM	Raman	EBSD
Mechanical	✓	✓	✓
Ion	✓	✓	✓
Laser	✓	✓	X

Moving forward, the most important diamond-containing ceramics can be sent out for mechanical polishing. While this method is the most time-intensive, the surface quality is sufficient for the entire suite of characterization techniques available (SEM, Raman, and EBSD/EDS). In-house techniques like ion or laser polishing can save some time and help down-select these most important samples. However, as previously discussed, there are limitations to the in-house polishing methods. Coupling these sample preparation methods will provide a thorough characterization suite for any new diamond composite materials. This will also be useful information for future small-scale mechanical testing where the surface can have a strong influence on the results.

5. References

1. United States Geological Survey (USGS). Industrial diamond statistics and information; 2019 [accessed 2019 Oct 1]. https://www.usgs.gov/centers/nmic /industrial-diamond-statistics-and-information.

2. Matthey B, Hohn S, Wolfrum AK, Muhle U, Motylenko M, Rafaja D, Michaelis A, Herrmann M. Microstructural investigation of diamond-SiC composites produced by pressureless silicon infiltration. Journal of the European Ceramic Society. 2017;37:1917–1928.

3. Herrmann M, Matthey B, Höhn S, Kinski I, Rafaja D, Michaelis A. Diamond-ceramic composites: new materials for a wide range of challenging applications. Journal of the European Ceramic Society. 2012;32:1915–1923.

4. Zhao Y, Qian J, Daemen LL, Pantea C, Zhang J, Voronin GA, Zerda TW. Enhancement of fracture toughness in nanostructured diamond-SiC composites. Applied Physics Letters. 2004;84:1356–1358.

5. Hird JR, Field JE. Diamond polishing. Proc R Soc Lond A. 2004;460:3547–3568.

6. Schuelke T, Grotjohn TA. Diamond polishing. Diamond and Related Materials. 2013;32:17–26.

7. Ji G, Tan Z, Shabadi R, Li Z, Grünewald W, Addad A, Schryvers D, Zhang D. Triple ion beam cutting of diamond/Al composites for interface characterization. Materials Characterization. 2014;89:132–137.

8. Bettonville. Diamond cutting laser machines. Konstancin (Poland): Bettonville [accessed 2019 Oct 1]. https://www.bettonville.com/.

9. Gaywala R. Laser cutting transforms the diamond processing industry. Industrial Laser Solutions for Manufacturing; 2015 July 14 [accessed 2019 Oct 1]. https://www.industrial-lasers.com/cutting/article/16485509/ laser-cutting-transforms-the-diamond-processing-industry.

10. Pimenov SM, Kononenko VV, Ralchenko VG, Konov VI, Gloor S, Lüthy W, Weber HP, Khomich AV. Laser polishing of diamond plates. Applied Physics A. 1999;69:81–88.

11. Gloor S, Lüthy W, Weber HP, Pimenov SM, Ralchenko VG, Konov VI, Khomich AV. UV laser polishing of thick diamond films for IR windows. Applied Surface Science. 1999;138-139:135–139.

12. Ozkan AM, Malshe AP, Railkar TA, Brown WD, Shirk MD, Molian PA. Femtosecond laser-induced periodic structure writing on diamond crystals and microclusters. Applied Physics Letters. 1999;75:3716–3718.

13. Wu Q, Ma Y, Fang R, Liao Y, Yu Q, Chen X, Wang K. Femtosecond laser-induced periodic surface structure on diamond film. Applied Physics Letters. 2003;82:1703–1705.

14. Sedao X, Maurice C, Garrelie F, Colombier J-P, Reynaud S, Quey R, Pigeon F. Influence of crystal orientation on the formation of femtosecond laser-induced periodic surface structures and lattice defects accumulation. Applied Physics Letters. 2014;104:171605.

15. Vorobyev AY, Guo C. Femtosecond laser-induced periodic surface structure formation on tungsten. Journal of Applied Physics. 2008;104:063523.

16. Young JF, Preston JS, van Driel HM, Sipe JE. Laser-induced periodic surface structure II. Experiments on Ge, Si, Al, and Brass. Phys Rev B. 1983;27:1155–1172.

17. Beard MA, Ghita OR, Evans KE. Using Raman spectroscopy to monitor surface finish and roughness of components manufactured by selective laser sintering. Journal of Raman Spectroscopy. 2011;42:744–748.

List of Symbols, Abbreviations, and Acronyms

CI	confidence index
CVD	chemical vapor deposited
EBSD	electron backscatter diffraction
EDS	energy dispersive spectroscopy
ID	identification
IPF	inverse pole figure
IQ	image quality
LIPSS	laser-induced periodic surface structure
SEM	scanning electron microscope
SiC	silicon carbide

1 (PDF)	DEFENSE TECHNICAL INFORMATION CTR DTIC OCA
1 (PDF)	CCDC ARL FCDD RLD CL TECH LIB
19 (PDF)	CCDC ARL FCDD RLW B L VARGAS-GONZALEZ FCDD RLW M B LOVE FCDD RLW MB D O'BRIEN C FOUNTZOULAS A GAYNOR G GAZONAS E HERNANDEZ D HOPKINS J LIGDA B POWERS T SANO T WALTER D MAGAGNOSC FCDD RLW ME M GOLT A DIGIOVANNI J LASALVIA S SILTON S COLEMAN W SHOULDERS